

Fenton Process for the Degradation of Methylene Blue using Different Nanostructured Catalysts

¹María del C Cotto-Maldonado, ¹José Duconge, ²Carmen Morant and ¹Francisco Márquez

¹Nanomaterials Research Group, School of Natural Sciences and Technology, University of Turabo, 00778-PR, USA

²Department of Applied Physics, Universidad Autónoma de Madrid, 28049-Cantoblanco, Madrid, Spain

Article history

Received: 15-03-2017

Revised: 17-03-2017

Accepted: 12-07-2017

Corresponding Author:

María del C Cotto-Maldonado

Nanomaterials Research Group, School of Natural Sciences and Technology, University of Turabo, 00778-PR, USA

Email: mcotto48@suagm.edu

Abstract: In many places of the world, water is a scarcity resource. The possibility of reusing water increases the relevance of developing different water treatment methods. The goal of this research was to determine if the photo-Fenton processes are efficient for the degradation of organic compounds, as a possible alternative for wastewater treatment. In order to carry out this study, different catalysts were characterized by different techniques (XRD, FE-SEM, SBET and TGA) and catalytic tests. Iron oxide nanowires (Fe₂O₃NWs) and a commercial catalyst (FeCl₂) were tested in the methylene blue photo-Fenton degradation reaction. The catalysts used were able to degrade the methylene blue and could eventually be used to remove contaminants from the water.

Keywords: Photo-Fenton Process, Methylene Blue, Iron Oxide Nanowires, Advanced Oxidation Processes

Introduction

One of the most discussed issues around the world is the water chemical pollution by organic, inorganic, bionutrients and microorganisms (Garriga I Cabo, 2007; UNEP *et al.*, 2002). In many regions of the world, water is a scarce resource and in these places the reuse of the water is a major issue (Marin *et al.*, 2007). The production and use of synthetic chemicals has experienced a significant increase over the past century and mankind is responsible for releasing many of the pollutants into the environment in their normal activities like industrial processes, wastewater discharges, overuse of pesticides, fertilizers, etc. (Ameta *et al.*, 2013).

Aromatic compounds are an important source of environmental pollution that reaches the atmosphere and groundwater, since they are widely used as intermediates in the production of pesticides, synthetic polymers and dyes (Huang *et al.*, 2010). The presence of these substances in the environment is worrisome, since they have carcinogenic, teratogenic and toxic properties (especially the azo dyes), they diminish the penetration of light through the water column and although it is not so relevant, they also affect aesthetically to nature (Houas *et al.*, 2001; Karadag *et al.*, 2006; Dafnopatidou *et al.*, 2007).

Effluents from the textile industry have high concentrations of organic and inorganic dyes which are

heavily colored, have a high Chemical Oxygen Demand (COD), fluctuate significantly in pH and are toxic to organisms (Abdelmalek *et al.*, 2006). Common techniques used to remove dyes include chemical, physical and biological processes (Dafnopatidou *et al.*, 2007). However, these conventional processes for the treatment of wastewater including the degradation of residual dyes are ineffective because these compounds have a high molecular weight and high biochemical stability due to the presence of aromatic rings in their structure (Panizza *et al.*, 2006; Ma *et al.*, 2007).

To maintain aesthetics and to reduce the environmental impact of industrial effluents, discoloration of the wastewater is necessary (Hussein Sharif Zein and Boccaccini, 2008). Currently, the most commonly used treatment methods for the removal of water pollutants are reverse osmosis, ion exchange technology, precipitation of materials, adsorption of pollutants by using activated carbon (charcoal) and biological degradation (Gupta *et al.*, 2004; Mezohegyi *et al.*, 2007). Other processes as Fenton, photochemistry, radiolysis or sonolysis generate highly reactive hydroxyl radicals for bleaching, finally arising to the mineralization of recalcitrant compounds (Ozen *et al.*, 2005). In the boom of the eco-conservation and the eco-friendly techniques to degrade the pollutants in water and wastewater, the Advance Oxidation Processes or AOPs are seen as alternative techniques (Gupta *et al.*, 2004) to the

traditional processes. The AOPs use chemical procedures based on the use of catalysts or photochemical compounds which generate highly reactive transient species as the hydroxyl radical which possesses high efficiency for the oxidation of organic compounds (Marin *et al.*, 2007; Mohabansi *et al.*, 2011; Salehi *et al.*, 2012; Samet *et al.*, 2012). AOPs have many advantages such as complete mineralization of the pollutant, are non-selective processes, are used in low concentration of contaminants and can be combined with other methods (Garriga I Cabo, 2007).

The Fenton reaction, as part of the AOPs, generates hydroxyl radicals. This process is clearly non selective (Ai *et al.*, 2007a) and represents a viable technique to degrade hazardous organic compounds (Barbusiński, 2005). Horstman Fenton and Jackson (1899) demonstrated the importance of iron and hydrogen peroxide during the oxidation of some substances. A characteristic of the Fenton process is that the reaction requires acid conditions to work more efficiently (pH ranging from 2 to 3) (Ai *et al.*, 2007a). According to Ai *et al.* (2007b), the Fenton reagent can be defined as the combination of hydrogen peroxide and iron (II) ($\text{Fe}^{2+}/\text{H}_2\text{O}_2$). Fenton-like reagent does not include iron (II) species and normally this term is used for the combination of $\text{Fe}^{3+}/\text{H}_2\text{O}_2$ although both reagents (Fenton and Fenton-like) are present during the reaction because both iron species are in equilibrium during the reaction. An alternative to the typical Fenton reactions based on the use of soluble $\text{Fe}^{2+}/\text{Fe}^{3+}$ species is the use of Fe^0 , as a supported or immobilized catalyst and hydrogen peroxide as oxidizer (Ai *et al.*, 2007b). Examples of possible reagents for environmental remediation include Fe^0 , Fe_3O_4 (magnetite) and Fe_2O_3 (maghemite) (Ai *et al.*, 2007b; Reza *et al.*, 2016).

Methylene Blue (MB) (Fig. 1) is a hetero-polyaromatic dye commonly used for printing cotton, as textile tannin and for coloring leather (Ma *et al.*, 2007; Salmin and Shamali, 2013). MB is also used in chemistry as a base-acid indicator and in the medical field.

In this research, we have studied the efficiency of the photo-Fenton degradation process of MB in aqueous solution. The results obtained point to the fact that these catalytic processes could be implemented in the efficient degradation of recalcitrant pollutants present in wastewater.

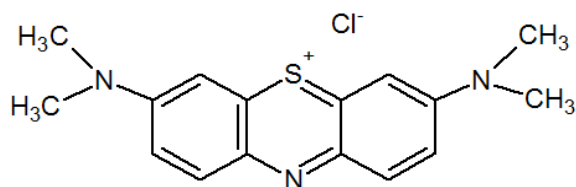


Fig. 1. Molecular structure of methylene blue

Experimental Section

Reagents

All chemicals used in this research were of analytical grade and were used as received without any further purification. Methylene Blue (MB) p.a. was provided by Sigma Aldrich. Isopropyl alcohol and ethyl alcohol (95% purity) were provided by Acros Organics. The iron substrate (99.999%) was provided by Good fellow (USA). Ferrous Chloride (99% purity) was provided by Fisher Scientific. Milli-Q water (18.2 M Ω .cm resistivity at 25°C) was used for all experiments.

Characterization Techniques

X-Ray powder Diffraction patterns (XRD) were collected using an X'Pert PRO X-ray diffractometer (PANalytical, The Netherlands) in the Bragg-Brentano geometry. The thermogravimetric analyses were done using a TGA Q-500 instrument (TA Instruments) under an inert atmosphere of nitrogen. The specific surface areas of the catalysts used in the present research were determined by the BET method using a Micromeritics ASAP 2020. The variation in magnetization and coercivity of the Fe_2O_3 NWs was determined by using a Lake Shore-7400 Vibrating Sample Magnetometer (VSM) at room temperature. Field emission scanning electron microscopy (FE-SEM) images were obtained using a JEOL JM-6400 microscope. High Resolution Transmission Electron Microscopy (HRTEM) images were recorded on a JEOL 3000 with an acceleration voltage of 300 kV. The Total Organic Carbon (TOC) concentration was determined by using both a Tekmar Dohmann, Phoenix 8000 UV-Persulfate TOC Analyzer and a Leco CHNS-932 Analyzer. The catalytic degradation of MB was studied by using UV-vis absorption (Varian Cary 3 spectrophotometer) and fluorescence (Varian Cary Eclipse spectrometer).

Synthesis of Iron Oxide Nanowires

Crystalline iron oxide nanowires were synthesized by a simple catalyst-free growth procedure. The iron substrates (Goodfellow, 99.999%) were thermally treated in a tubular oven. In a standard synthesis procedure, the iron substrates were incorporated into the furnace after being degreased by rinsing with acetone and isopropanol. The thermal treatment consists of a ramp-up rate of 25°C/min to the final temperature of 500°C, followed by one hour plateau, in flowing air (300 mL/min); and finally a cooling ramp rate of 25°C/min in vacuum (Fig. 2) (Bonilla *et al.*, 2011).

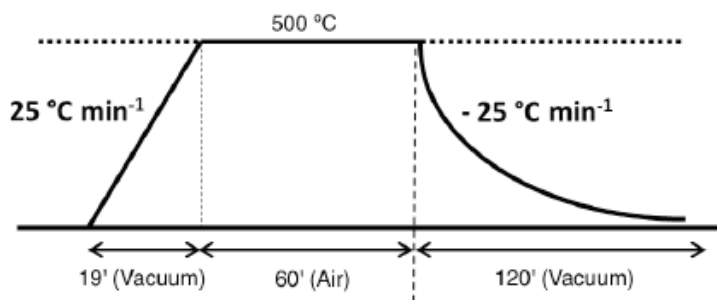


Fig. 2. Scheme of the thermal treatment

Results and Discussion

Material Characterization-Iron Oxide Nanowires (Fe_2O_3 NWs)

Fe_2O_3 NWs were synthesized according to the procedure described above. The SEM images of the synthesized samples are shown in Fig. 3. Iron oxide nanowires are characterized by having a high aspect ratio, with lengths above 5 microns and diameters below 100 nm. However, in preliminary studies, it was found that Fe_2O_3 NWs become thicker (with diameters that can be three times greater), when the synthesis temperature increases above 600°C, indicating the effect of temperature on the morphology of these nanostructures. The BET surface analysis revealed an unexpectedly high specific surface area (S_{area}) of 180 m² g⁻¹ (Table 1) which has been related to the high aspect ratio of this material. TG analysis revealed only a weight loss of 3.62% at 520°C (Table 1), indicating that iron nanowires do not possess porosity capable of absorbing an appreciable amount of water or other solvents. This result clearly points to the fact that the specific area of this material is due to the high aspect ratio and not to a possible porosity produced during the synthesis of the material.

The morphology and size of the as-synthesized Fe_2O_3 NWs was also investigated by TEM. Figure 4 shows a TEM image of an isolated Fe_2O_3 nanowire (a) and the corresponding Selected Area Electron Diffraction Pattern (SAED) (b). As can be seen there, the surface of the nanowire does not have a smooth appearance, showing small particles that could also contribute to the surface area value measured for this material. The SAED (Fig. 3b) is consistent with a single crystal structure. The halo-rings could be due to the presence of small crystals on the nanowire surface.

Magnetic properties of the as-synthesized Fe_2O_3 NWs were also characterized. Figure 5 shows the hysteresis loop of the iron nanowires at room temperature. The coercivity value obtained for this material was 20.485 G, with saturation Magnetization (M_s) of 22.376 emu g⁻¹, indicating a high ferromagnetic behavior (Wu *et al.*, 2010).

Fe_2O_3 NWs was also characterized by XRD. Figure 6 shows the diffractions patterns corresponding to samples synthesized in oxidative atmosphere (in flowing air) at 500°C (4a) and 700°C (4b). The results indicated the presence of highly crystalline magnetite (Fe_3O_4). However, as can be seen in Fig. 6, some small differences are observed as a function of the synthesis temperature, showing possible changes in the structure (phase) and crystallinity (Bonilla *et al.*, 2011).

Iron oxide as hematite phase (α - Fe_2O_3) was not observed, due to the lack of peaks corresponding to reflections (210) and (211), that are always present in this crystallographic phase (Daou *et al.*, 2006).

Ferrous Chloride ($FeCl_2$)

Ferrous chloride ($FeCl_2$, Fisher Scientific, 99%) was used in this research to compare its efficiency with respect to the synthesized catalyst. The thermogravimetric analysis of this compound established a weight loss of approximately 16.14% (Table 1). The TG curve showed a single step of weight loss and this behavior was attributed to the removal of water molecules adsorbed on the surface of the compound (Niederberger *et al.*, 2002). The specific surface area (S_{area}), measured by the BET method, was 55 m² g⁻¹ (Table 1).

Catalytic Tests

Photo-Fenton degradation catalytic processes were carried out using a cylindrical reactor (semi-batch type), with continuous stirring, which was located in the center of a solar simulator as irradiation source. The experimental setup was composed by two annular white bulb lights with a total irradiation power of 60 watts. A vessel of 1 L was used during the irradiation of the sample. The sample was mechanically stirred to maintain a homogeneous mixture during the irradiation of the sample. Before the irradiation, the selected catalyst was dispersed in the solution and kept in the dark under stirring for 30 min (Hong *et al.*, 2009) to ensure substrate-surface equilibrium (Zhou *et al.*, 2010).

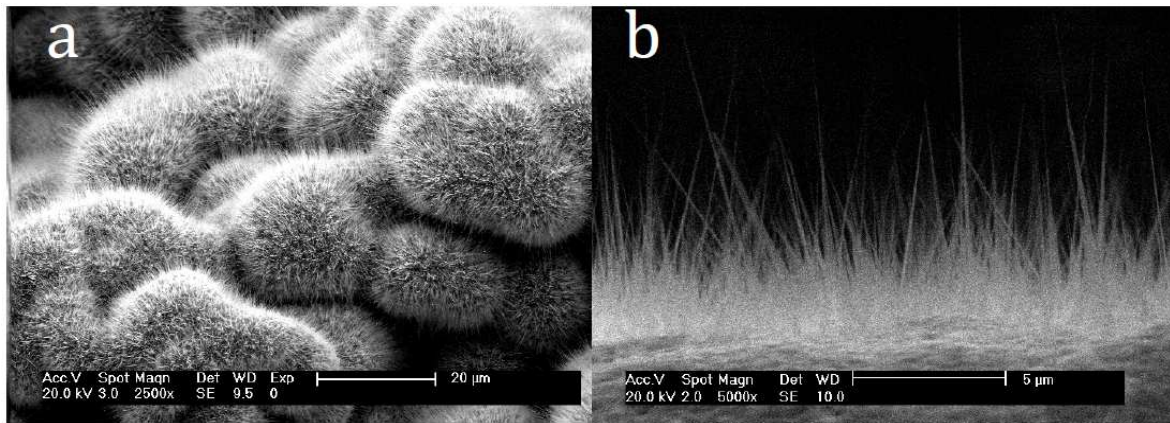


Fig. 3. SEM images of the as-synthesized iron oxide nanowires: Top-view (a) and side view image (b)

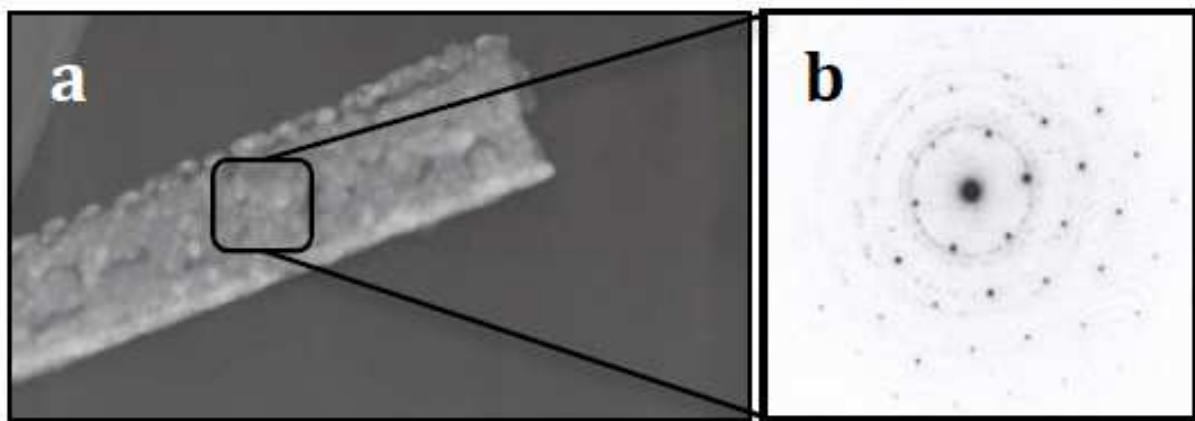


Fig. 4. TEM image of an isolated $\text{Fe}_2\text{O}_3\text{NW}$ (a), and the corresponding SAED pattern (b)

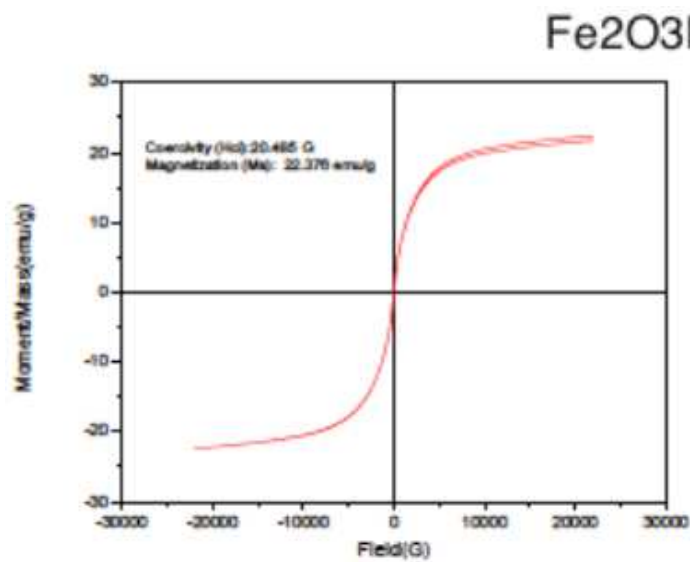


Fig. 5. Magnetic susceptibility of as-synthesized $\text{Fe}_2\text{O}_3\text{NWs}$, measured at 25°C

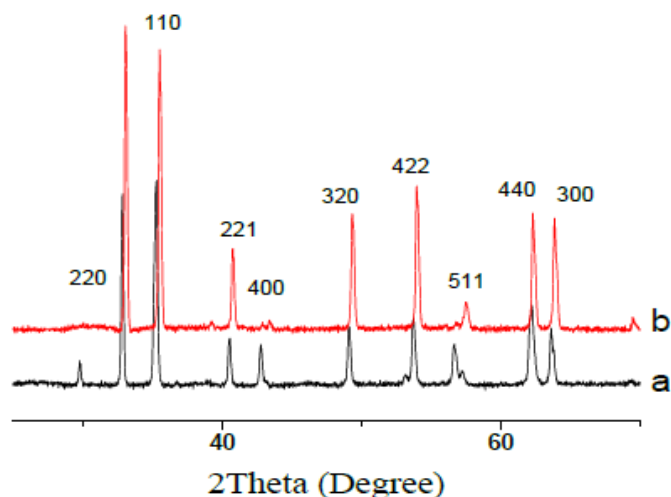


Fig. 6. XRD diffraction patterns of Fe₂O₃NWs synthesized at 500°C (a) and 700°C (b) at atmospheric pressure in flowing air

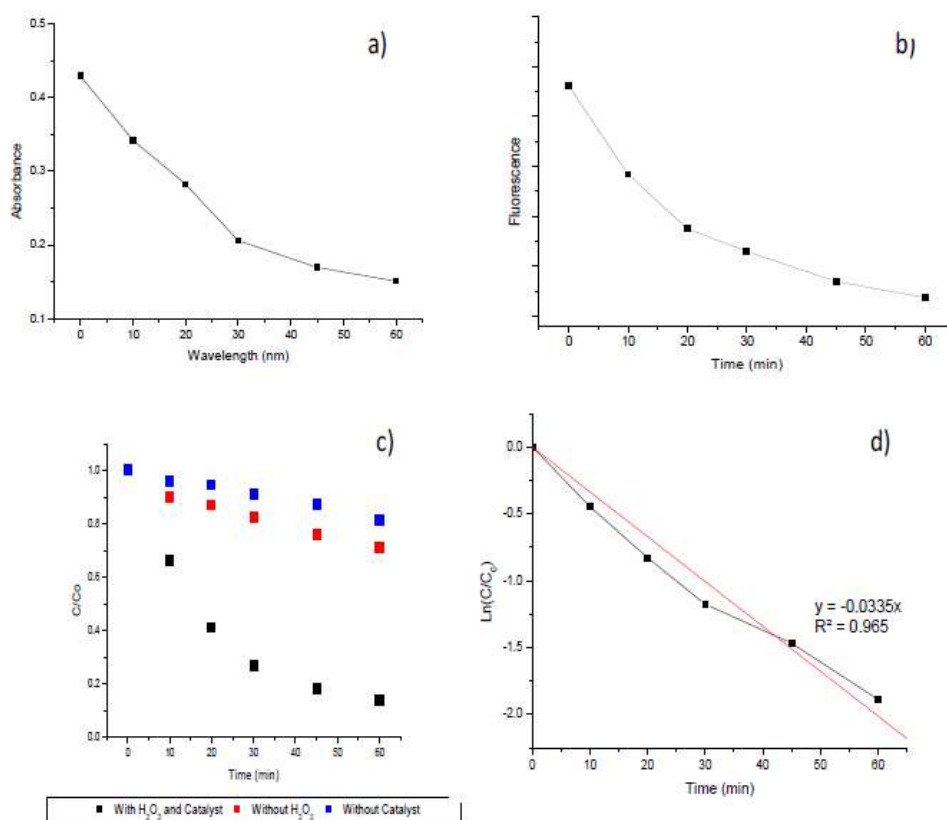


Fig. 7. Decrease of the UV-visible absorption (a), fluorescence (b), TOC (c) and graph of the pseudo-first order reaction rate and regression line (d), during the photocatalytic degradation process of MB using Fe₂O₃NWs as catalyst

Table 1. Surface area (BET) and thermogravimetric analysis of synthesized and commercial catalysts

Sample	SBET (m ² g ⁻¹)	TGA (%)
Fe ₂ O ₃ NWs	180	3.62
FeCl ₂ *	55	16.14

*Commercial catalyst

All systems were covered to avoid any further irradiation on the sample. In this way, only the light from the solar simulator was able to reach the sample. Hydrogen peroxide was added to the sample batch to increase the oxygen source during the reaction, avoiding the decrease of the catalytic activity during the reaction

due to lack of oxygen (Cotto-Maldonado, 2012). The volume of hydrogen peroxide added to the batch, the concentration of the dye and the catalyst concentration were 0.1 mL, 10^{-5} M and 0.6 gL^{-1} , respectively (Velegraki and Mantvinos, 2008; Asiri *et al.*, 2011; Cotto-Maldonado, 2012). A 10 mL-aliquot of the reaction mixture was extracted every 10 min and a dilution (1:5, v/v) was prepared to record the UV and fluorescence spectra and to determine the TOC concentration.

Fluorescence intensity and UV-vis absorption were measured at $\lambda = 665 \text{ nm}$ and $\lambda = 670 \text{ nm}$, respectively. TOC was used as a complementary technique to spectroscopy. Figure 7 shows the results obtained with $\text{Fe}_2\text{O}_3\text{NWs}$ as catalyst. As can be seen in Fig. 7a and 7b, the absorbance and fluorescence intensity are reduced by about 80% of the initial value, confirming the degradation of the compound. This result was also verified by total organic carbon measurements. Figure 7c shows the evolution of TOC at different times under different experimental conditions. Under the same reaction conditions as those used for monitoring

degradation by UV-vis absorption spectroscopy and fluorescence, the greatest reduction in carbon level was observed (black dots). In the absence of catalyst (blue dots), the degradation is minimal, probably produced by oxidation of the MB in the presence of H_2O_2 . When the reaction is carried out using only the oxygen present in water (red dots), the reaction proceeds very weakly until the oxygen present in the solution is exhausted, resulting in minimal MB degradation.

In the presence of FeCl_2 as catalyst and under similar experimental reaction conditions, the MB undergoes a degradation slightly higher than that observed with $\text{Fe}_2\text{O}_3\text{NWs}$ (Fig. 8).

Table 2 shows the percent of degradation (based on the decrease in TOC concentration). According with the data presented there, the FeCl_2 has the highest degradation rate during the photo-Fenton process, reaching a value of 92%. The high efficiency of the FeCl_2 as catalyst could be due to the high solubility of this catalyst with respect to $\text{Fe}_2\text{O}_3\text{NWs}$.

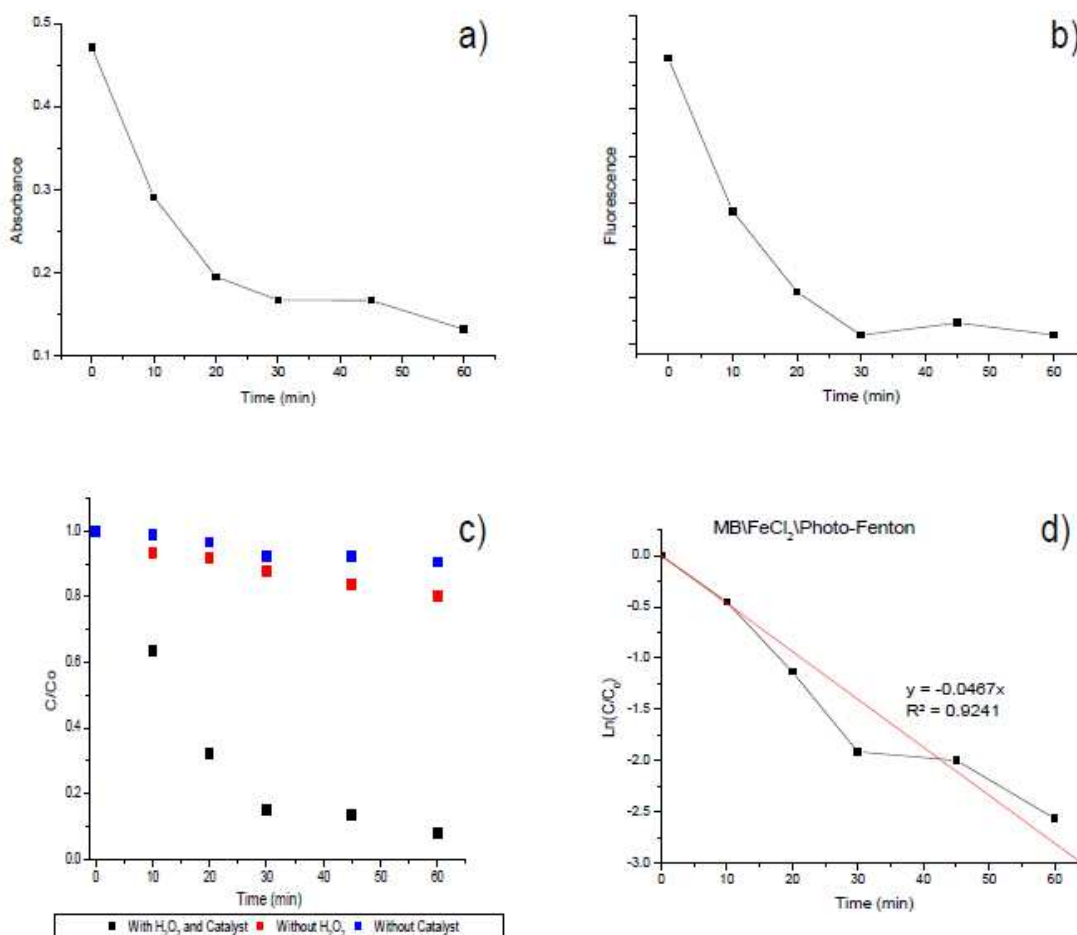


Fig. 8. Decrease of the UV-visible absorption (a), fluorescence (b), TOC (c), and graph of the pseudo-first order reaction rate and regression line (d), during the photocatalytic degradation process of MB using FeCl_2 as catalyst

Table 2. Percent degradation and kinetic reaction rates of MB in the Photo-Fenton process

	Catalysts	
	Fe ₂ O ₃ NWs	FeCl ₂
Degradation (%)	86 %	92 %
Rate constant (<i>k</i>)	5.58×10 ⁻⁴ s ⁻¹	7.78×10 ⁻⁴ s ⁻¹

The photocatalytic activity was quantitatively evaluated by calculating the pseudo first-order rate constants (*k*) according to the following equation (Wang *et al.*, 2006; Asiri *et al.*, 2011; Salehi *et al.*, 2012):

$$\ln(C_0 / C) = kt$$

where, *C*₀ and *C* are the initial concentration of MB and its concentration at the time *t*, respectively. The semilogarithmic plots of the concentrations Vs time were adjusted using a linear regression to determine the rate constant (Fig. 7d and 8d). Table 2 shows the *k* values for the degradation reaction of the MB during the photo-Fenton process. The kinetic rate represents a measure of the catalytic activity. Therefore, the larger this magnitude, the greater the catalytic activity of the system. As can be seen in Table 2, both catalysts (Fe₂O₃NWs and FeCl₂) have kinetic rates of the same order of magnitude, although higher in FeCl₂. The higher efficiency shown by FeCl₂ may be due to the solubility of the catalyst in water. In fact, unlike Fe₂O₃NWs which is not soluble in water and can be recovered by centrifugation, once FeCl₂ is used, it cannot be recovered.

Conclusion

Fe₂O₃NWs was synthesized by heat treatment of an iron substrate in air. The material obtained was recovered and characterized by SEM, TEM, TGA and magnetometry. The activity of this catalyst has been compared with that of the commercial catalyst FeCl₂, studying the efficiency of the photo-Fenton degradation process of a stable organic dye (methylene blue) in water. As a result, the activity of both catalysts was comparable, although a higher efficiency was obtained in the commercial catalyst (FeCl₂). This result has been justified as possibly due to the higher solubility of FeCl₂ in water. The activity of Fe₂O₃NWs, although this material is not soluble, could be due to its high specific area, compared to FeCl₂.

The use of photo-Fenton degradation reactions opens a world of possibilities that in the future could be implemented at an industrial level for the abatement of organic pollutants in inland waters.

Acknowledgement

This work was supported by MINECO under Grant ENE2014-57977-C2-1-R. Financial support from the U.S. Department of Energy, through the Massie Chair Project at Universidad del Turabo and from the U.S. Department of Defense under Grant W911NF-14-1-0046 is gratefully acknowledged.

Author's Contributions

All authors contributed equally to this work.

Ethics

Nothing to declare.

References

- Abdelmalek, F., M.R. Ghezzar, M. Belhadj, A. Addou and J.L. Brisset, 2006. Bleaching and degradation of textile dyes by nonthermal plasma process at atmospheric pressure. *Ind. Eng. Chem. Res.*, 45: 23-29. DOI: 10.1021/ie050058s
- Ai, Z., L. Lu, J. Li, L. Zhang and J. Qiu *et al.*, 2007a. Fe@Fe₂O₃ core-shell nanowires as the iron reagent. 2. An efficient and reusable sono-fenton system working at neutral pH. *J. Phys. Chem. C.*, 111: 7430-7436. DOI: 10.1021/jp070412v
- Ai, Z., L. Lu, J. Li, L. Zhang and J. Qiu *et al.*, 2007b. Fe@Fe₂O₃ core-shell nanowires as iron reagent. 1. Efficient degradation of rhodamine B by a novel sono-fenton process. *J. Phys. Chem. C.*, 111: 4087-4093. DOI: 10.1021/jp065559l
- Ameta, A., R. Ameta and M. Ahuja, 2013. Photocatalytic degradation of methylene blue over ferric tungstate. *Sci. Revs. Chem. Commun.*, 3: 172-180.
- Asiri, A.M., M.S. Al-Amoudi, T.A. Al-Talhi and A.D. Al-Talhi, 2011. Photodegradation of rhodamine 6G and phenol red by nanosized TiO₂ under solar irradiation. *J. Saudi Chem. Soc.*, 15: 121-128. DOI: 10.1016/j.jscs.2010.06.005
- Barbusiński, K., 2005. The modified Fenton process for decolorization of dye wastewater. *Polish J. Environ. Stud.*, 14: 281-285.
- Bonilla, C., A. García, J. Ducongé, T. Campo and E. Elizalde *et al.*, 2011. Synthesis and characterization of crystalline Fe₂O₃ nanowires by oxidation of iron substrates. Proceedings of the 43rd IUPAC World Chemistry Congress, (WCC' 11), San Juan, PR, USA.
- Cotto-Maldonado, M.C., 2012. Heterogeneous catalysis Applied To Advanced Oxidation Processes (AOPs) for degradation of organic pollutants. A Dissertation submitted in partial fulfillment of the requirements for the degree of Doctor of Philosophy, Universidad del Turabo, Gurabo, Puerto Rico, USA.

- Dafnopatidou, E.K., G.P. Gallios, E.G. Tsatsaroni and N.K. Lazaridos, 2007. Reactive dyestuffs removal from aqueous solutions by flotation, possibility of water reuse and dyestuff degradation. *Ind. Eng. Chem. Res.*, 46: 2125-2132.
DOI: 10.1021/ie060993v
- Daou, T.J., G. Pourroy, S. Begin-Colin, J.M. Greneche and C. Ulhaq-Bouillet *et al.*, 2006. Hydrothermal synthesis of monodisperse magnetite nanoparticles. *Chem. Mater.*, 18: 4399-4404.
DOI: 10.1021/cm060805r
- Garriga I Cabo, C. 2007. Estrategias de optimizacion de procesos de descontaminacion de efluentes acuosos y gaseosos mediante fotocatalisis heterogenea. [Strategies for the optimization of the decontamination of aqueous and gaseous effluents using heterogeneous photocatalysis]. dissertation. Canarias, Gran Canarias, Spain. Spanish.
- Gupta, V.K., A.I. Suhas and V.K. Saini, 2004. Removal of rhodamine B, fast green and methylene blue from wastewater using red mud, an aluminum industry waste. *Ind. Eng. Chem. Res.*, 43: 1740-1747.
DOI: 10.1021/ie034218g
- Hong, R.Y., J.H. Li, L.L. Chen, D.Q. Liu and H.Z. Li *et al.*, 2009. Synthesis, surface modification and photocatalytic property of ZnO nanoparticles. *Powder Technol.* 189:426-432.
DOI: 10.1016/j.powtec.2008.07.004
- Horstman Fenton, H.J and H.J. Jackson, 1899. The oxidation of polyhydric alcohols in presence of iron. *J. Chem. Soc. Trans.*, 75: 1-11.
DOI: 10.1039/CT8997500001
- Houas, A., H. Lachheb, M. Ksibi, E. Elaloui and C. Guillard *et al.*, 2001. Photocatalytic degradation pathway of methylene blue in water. *Applid Catal. B: Environ.*, 31: 145-157.
DOI: 10.1016/S0926-3373(00)00276-9
- Huang, J., Y. Cui and X. Wang, 2010. Visible light-sensitive ZnGe oxynitride catalysts for the decomposition of organic pollutants in water. *Environ. Sci. Technol.*, 44: 3500-3504.
DOI: 10.1021/es1001264
- Hussein Sharif Zein, S. and A.R. Boccaccini, 2008. Synthesis and characterization of TiO₂ coated multiwalled carbon nanotubes using a sol gel method. *Material and Interfaces. Ind. Eng. Chem. Res.*, 47: 6598-6606. DOI: 10.1021/ie701770q
- Karadag, D., S. Tok, E. Akgul, K. Ulucan and H. Evden *et al.*, 2006. Combining adsorption and coagulation for the treatment of azo and anthraquinone dyes from aqueous solution. *Ind. Eng. Chem. Res.*, 45: 3969-3973.
DOI: 10.1021/ie060164+
- Ma, H., Q. Zhuo and B. Wang, 2007. Characteristics of CuO-MoO₃-P₂O₅ catalyst and its Catalytic Wet Oxidation (CWO) of dye wastewater under extremely mild conditions. *Environ. Sci. Technol.*, 41: 7491-7496. DOI: 10.1021/es071057p
- Marin, J.M., J. Montoya, E. Monsalve, C.F. Granda and L.A. Rios *et al.*, 2007. Degradación de naranja de metilo de un nuevo fotorreactor solar de placa plana con superficie corrugada [Degradation of Methyl Orange by a new solar photoreactor]. *Scientia Et Tech.*, 13: 435-440.
- Mezohegyi, G., A. Kolodkin, U.I. Castro, C. Bengoa and F. Stuber *et al.*, 2007. Effective anaerobic decolorization of azo dye acid orange 7 in continuous upflow packed-bed reactor using biological activated carbon system. *Ind. Eng. Chem. Res.*, 46: 6788-6792. DOI: 10.1021/ie061692o
- Mohabansi, N.P., V.B. Patil and N. Yenkie, 2011. A comparative study on photo degradation of methylene blue dye effluent by advanced oxidation process by using TiO₂/ZnO photo catalyst. *Rasayan J. Chem.*, 4: 814-819.
- Niederberger, M., M.H. Bartl and G.D. Stucky, 2002. Benzyl alcohol and titanium tetrachloride-a versatile reaction system for the nonaqueous and low-temperature preparation of crystalline and luminescent titania nanoparticles. *Chem. Mater.*, 14: 4364-4370. DOI: 10.1021/cm021203k
- Ozen, A.S., V. Aviyente, G. Tezcanli-Guyer and N.H. Ince, 2005. Experimental and modeling approach to decolorization of azo dyes by ultrasound: Degradation of the hydrazone tautomer. *J. Phys. Chem. A.*, 109: 3506-3516.
DOI: 10.1021/jp046374m
- Panizza, M., A. Barbucci, R. Ricotti and G. Cerisola, 2006. Electrochemical degradation of methylene blue. *Separat. Purificat. Technol.*, 54: 382-387.
DOI: 10.1016/j.seppur.2006.10.010
- Reza, K.M., A. Kurny and F. Gulshan, 2016. Photocatalytic degradation of methylene blue by magnetite + H₂O₂ + UV process. *Int. J. Environ. Sci. Dev.*, 7: 325-329.
DOI: 10.7763/IJESD.2016.V7.793
- Salehi, M., H. Hashemipour and M. Mirzaee, 2012. Experimental study of influencing factors and kinetics in catalytic removal of methylene blue with TiO₂ nanopowder. *Am. J. Environ. Eng.*, 2: 1-7.
DOI: 10.5923/j.ajee.20120201.01
- Salmin, S. and A. Shamali, 2013. Photocatalytic degradation of methylene blue in the presence of TiO₂ catalyst assisted solar radiation. *Austral. J. Basic Applied Sci.*, 7: 172-176.

- Samet, Y., E. Hmani and R. Abdelhédi, 2012. Fenton and solar photo-Fenton processes for the removal of chlorpyrifos insecticide in wastewater. *Water SA.*, 38: 537-542.
- UNEP, UNICEF and WHO, 2002. Children in the New Millenium: Environmental Threats to Children. United Nations Environment Program, United Nations Childrens Fund and World Health Organization.
- Velegraki, T. and D. Mantzavinos, 2008. Conversion of benzoic acid during TiO₂-mediated photocatalytic degradation in water. *Chem. Eng. J.*, 140: 15-21. DOI: 10.1016/j.cej.2007.08.026.
- Wang, X.H., J.G. Li, H. Kamiyama, Y. Moriyoshi and T. Ishigaki, 2006. Wavelength-Sensitive Photocatalytic Degradation of Methyl Orange in Aqueous Suspension over Iron (III)-doped TiO₂ Nanopowders under UV and Visible Light Irradiation. *J. Phys. Chem. B*, 110: 6804-6809.
- Wu, W., X. Xiao, S. Zhang, J. Zhou and L. Fan *et al.*, 2010. Large-scale and controlled synthesis of iron oxide magnetic short nanotubes: Shape evolution, growth mechanism and magnetic properties. *J. Phys. Chem. C.*, 114: 16092-16103. DOI: 10.1021/jp1010154
- Zhou, W., H. Liu, J. Wang, D. Liu and G. Du *et al.*, 2010. Ag₂O/TiO₂ nanobelts heterostructure with enhanced Ultraviolet and Visible photocatalytic activity. *Applied Mater. Interf.*, 2: 2385-2390. DOI: 10.1021/am100394x